Effect of Chemical Kinetics on Feasible Splits for Reactive Distillation

Nitin Chadda, Michael F. Malone, and Michael F. Doherty
Dept. of Chemical Engineering, University of Massachusetts, Amherst, MA 01003

Feasible direct and indirect sharp splits for multicomponent single-feed continuous reactive distillation are predicted with a model, in which each column section is represented by a series of cocurrent isobaric flashes. In the limits of no reaction and equilibrium chemical reaction, the model reduces to conventional models for distillation lines, and each column section can be represented by the same equations. At intermediate reaction rates, however, the models for the column sections differ, and new results for fixed points and feasible products are obtained. A bifurcation study shows the limits of feasibility, including the influence of flow rate, catalyst level and holdup. Unlike distillation without reaction, limited ranges of feasibility in all of these variables are found. The method has been applied to five examples, one of which is described in detail. Feasibility predictions are validated by column simulations.

Introduction

Reactive distillation is potentially attractive whenever there is a liquid-phase reaction that involves an excess of reactant. In addition to potential reduced capital and energy costs, reactive distillation can lead to higher conversions by overcoming chemical equilibrium constraints. For multiple reactions where an intermediate is the desired product, reactive distillation may also provide higher selectivities. This is achieved by taking advantage of a separation that suppresses side reactions. In some cases the reaction also has the effect of "reacting away" some of the azeotropes, thereby simplifying the phase behavior and avoiding an expensive separation (Doherty and Buzad, 1992).

For a conceptual design of reactive distillation, systematic methods are needed for deciding its feasibility. We use geometric methods that have been used extensively to assess the feasibility for nonreactive distillation. For nonreactive distillation, a number of algorithms can be used to find the feasible splits. Stichlmair and Herguijuela (1992) calculate the products at total reflux, while Wahnshafft et al. (1992) and Fidkowski et al. (1993) use pinch tracking techniques to estimate the feasible products for finite as well as total reflux. These methods rely on geometric visualization, so have been applied to ternary mixtures. Algorithms building on these ideas, but that do not rely on visualization, are described by Safrit and Westerberg (1997) and Rooks et al. (1998). These methods can also be applied in the limit of reaction equilibrium using transformations of the compositions that have properties similar to those of mole fractions in nonreactive mixtures (Barbosa and Doherty, 1988; Ung and Doherty, 1995; Espinosa et al., 1995). These is a one-to-one correspondence between the real mole fractions and the transformed variables at chemical equilibrium.

Such one-to-one transformations are not known for kinetically controlled reactive distillation, although some aspects of these transforms remain useful in the kinetic regime. Studies at finite rates of reaction are important because most reactive distillation devices operate in this regime. There are several approaches available that capture some of the effects of finite reaction rates, such as, geometric design methods (Buzad and Doherty, 1994, 1995; Okasinski and Doherty, 1998); mixed integer nonlinear programming (MINLP) methods (Ciric and Gu, 1994; Papalexandri and Pistikopoulos, 1996; Ismail et al., 1999); attainable-region methods (Nisoli et al., 1997; McGregor et al., 1997); residue-curve/bifurcation methods (Rev, 1993; Venimadhavan et al., 1995, 1999; Thiel et al., 1997); difference-point methods (Lee et al., 2000a,b). However, there are few tools that assess the feasibility of reactive mixtures in the kinetic regime. Giessler et al. (1998,

Correspondence concerning this article should be addressed to M. F. Doherty at this current address: Dept. of Chemical Engineering, Univ. of California, Santa Barbara, CA 93106-5080.

1999) use static analysis to determine the feasibility of reactive columns operated with large internal flows. Chadda et al. (2000) generate feasible product regions at finite rates of reaction for ternary systems. However, that method cannot be extended to treat a larger number of components or multiple reactions.

In this article, we describe an algorithm for predicting feasible splits for continuous single-feed reactive distillation that is not limited by the number of reactions are components. The method described here uses minimal information to determine the feasibility of reactive columns: (1) phase equilibrium between the components in the mixture, (2) a reaction-rate model, and (3) feed specification. This is based on a bifurcation analysis of the fixed points for a cocurrent flash-cascade model. Unstable nodes ("light species") and stable nodes ("heavy species") in the flash-cascade model are candidate distillate and bottoms products, respectively, from a reactive distillation column. Therefore, we focus our attention on those splits that are equivalent to the "direct" and "indirect" *sharp splits* in nonreactive distillation. One of the products in these sharp splits could be a pure component, an azeotrope, or a kinetic pinch point; the other product will be in material balance with the first.

The proposed algorithm is based on

1. A bifurcation study to predict the distillate and bottoms products for the entire range of reaction rates from the limit of no reaction to the limit of chemical equilibrium. This provides a global view of the *sharp-split* products from a continuous reactive distillation at all rates of reaction.

2. Flash calculations and the application of the *lever rule* (overall mass balance relating the feed, distillate, and bottoms product streams) to predict feasible sharp splits for a given feed condition.

We also demonstrate that the feasible sharp splits predicted by the algorithm are in good agreement with column simulations. Thus, this algorithm can be used effectively to quickly estimate feasible sharp splits for continuous single-feed reactive distillation.

Flash-Cascade Model

In a distillation column, each section (rectifying or stripping) can be effectively represented by a countercurrent cascade of flashes. This cascade can be simplified for the purpose of estimating feasible product compositions, by removing the countercurrent recycles of liquid and vapor flows among successive flash units, leaving the cocurrent arrangement shown in Figure 1. The compositions of the liquid and vapor streams in the flash-cascade arrangement are close to those of the countercurrent cascade and by extension, to those in a column section. The two arrangements (countercurrent vs. cocurrent) differ mainly in that the recovery of the key components in the countercurrent cascade is much higher than in the flash-cascade arrangement (such as Henley and Seader, 1981, sec. 7.6). In a feasibility analysis, it is the product compositions that we are trying to estimate, so we use the simpler cocurrent flash cascades to study the feasibility of reactive mixtures in continuous columns.

In this section we formulate the reactive flash model for an equimolar chemistry. Next, we hypothesize a condition under which the trajectories of the flash cascade model lie in the

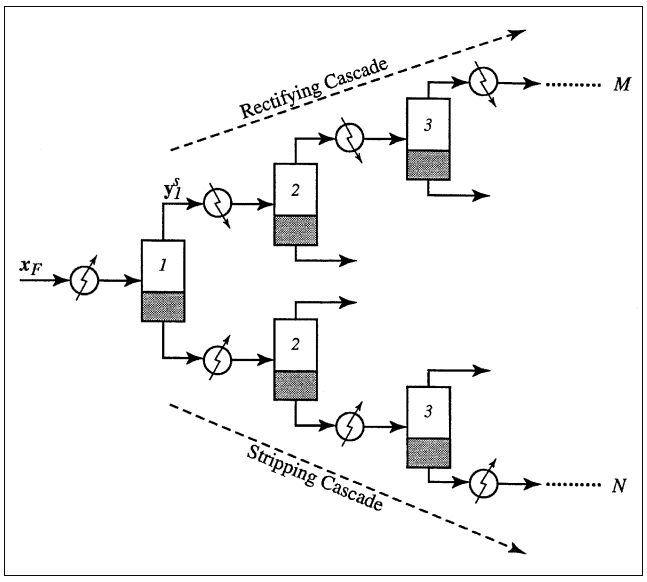

Figure 1. Cocurrent flash-cascades arrangement.

The top half is the rectifying cascade, and the bottom half is the stripping cascade.

feasible product regions for continuous reactive distillation. This hypothesis is tested for an example mixture at different rates of reaction. The fixed-point criteria for the flash cascade are derived and a bifurcation analysis shows the sharp-split products from a continuous reactive distillation.

The cocurrent flash-cascade arrangement is shown in Figure 1. There are two sections. In the rectifying cascade, vapor from each flash reactor is partially condensed and fed to the next unit. This vapor cascade is similar to the rectifying section of a continuous distillation column but without any liquid recycle. The opposite is done for the stripping cascade shown in the bottom half of the figure, where the liquid stream from each flash device is partially vaporized and sent as feed to the next unit in the series.

Each flash device in Figure 1 is a two-phase CSTR reactor-separator with the chemical reaction occurring only in the liquid phase. For simplicity we begin with a single reaction, an equimolar chemistry (see Appendix A for a more general model), a saturated liquid feed, and steady-state conditions. The flash devices operate under isobaric conditions, so that the temperature changes from stage to stage according to the boiling point of the stage composition. We use mole fractions and activity-based kinetic models for reasons explained in Venimadhavan et al. (1994) and Nisoli et al. (1997).

The overall mass balance for the jth unit in the stripping cascade, in Figure 2, is

$$L_{j-1} = V_j + L_j \qquad (j = 1, \ldots, N). \tag{1}$$

The material balance for the ith component is

$$L_{j-1}x_{i,j-1} = V_j y_{i,j} + L_j x_{i,j} - \nu_i k_f H_j r(\boldsymbol{x}_j) \qquad (i = 1, \ldots, c-1) \qquad (j = 1, \ldots, N), \tag{2}$$

where L and V are liquid and vapor molar flows; x_i and y_i

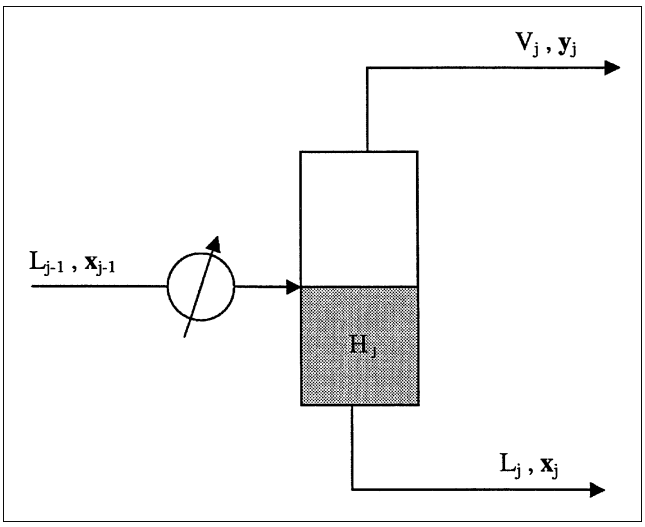

Figure 2. *j*th Flash in the stripping cascade.

are the liquid and vapor-phase mole fractions for component i; ν_i is the stoichiometric coefficient for component i; k_f is the forward rate constant with the dimensions of reciprocal time; H_j is the molar liquid holdup in the jth flash unit; and $r(\boldsymbol{x})$ is the reaction driving force:

$$r(\boldsymbol{x}) = \left(\prod_{\text{reactants}} a_i^{-\nu_i} - \prod_{\text{products}} \frac{a_i^{\nu_i}}{K_{\text{eq}}} \right), \tag{3}$$

where K_{eq} is the chemical equilibrium constant and a_i is the activity for component i. For liquid-phase reactions, activities are represented by the product of the activity coefficient, γ_i, and the liquid-phase composition, $a_i = \gamma_i x_i$.

Eliminating L_j from Eq. 2 leads to

$$x_{i,j-1} - x_{i,j} = \frac{V_j}{L_{j-1}}(y_{i,j} - x_{i,j}) - \nu_i k_f \frac{H_j}{L_{j-1}} r(\boldsymbol{x}_j) \qquad (i = 1, \ldots, c-1) \qquad (j = 1, \ldots, N) \tag{4}$$

We define two dimensionless parameters:

1. $\phi_j = V_j/L_{j-1}$, the fraction of feed vaporized in the jth unit.

2. $Da_j = (H_j/L_{j-1})/(1/k_{f,\text{ref}})$, the Damköhler number for unit j. This is the ratio of the characteristic liquid residence time to a characteristic reaction time (Damköhler, 1939). The forward rate constant, $k_{f,\text{ref}}$, is at a reference temperature, T_{ref}. No reaction occurs in the limit of $Da_j \to 0$, and reaction equilibrium is achieved as $Da_j \to \infty$. At intermediate Da_j, the stage operates in the kinetically controlled regime.

Incorporating ϕ_j and Da_j in Eq. 4, we find

$$x_{i,j-1} - x_{i,j} = \phi_j(y_{i,j} - x_{i,j}) - \nu_i \left(\frac{k_f}{k_{f,\text{ref}}} \right) Da_j r(\boldsymbol{x}_j) \qquad (i = 1, \ldots, c-1) \qquad (j = 1, \ldots, N), \tag{5}$$

where ϕ_j and Da_j are two independent parameters for each flash unit. We study the case where

1. The same fraction of feed is vaporized in each stage:

$$\phi_1 = \phi_2 = \cdots = \phi_j = \cdots = \phi_N = \phi. \tag{6}$$

2. Each flash stage has the same residence time:

$$Da_1 = Da_2 = \cdots = Da_j = \cdots = Da_N = Da. \tag{7}$$

These two assumptions imply that the vapor rate and the liquid holdup both decrease along the cascade for a fixed-feed flow rate. This produces a policy of decreasing vapor rate along the cascade similar to a decreasing vapor rate policy in simple (batch) distillation, which keeps the instantaneous value of Da approximately constant (Venimadhavan et al., 1994).

The model for the stripping cascade becomes

$$x_{i,j-1} = \phi y_{i,j} + (1-\phi)x_{i,j} - \nu_i \left(\frac{k_f}{k_{f,\text{ref}}} \right) Da\, r(\boldsymbol{x}_j) \qquad (i = 1, \ldots, c-1) \qquad (j = 1, 2, \ldots, N), \tag{8}$$

where $\boldsymbol{x}_0 = \boldsymbol{x}_F$.

It is convenient to introduce a dimensionless parameter (Venimadhavan et al., 1999)

$$D = \left(\frac{Da}{1 + Da} \right), \tag{9}$$

where D varies from 0 for the case of no reaction to unity in the limit of reaction equilibrium.

Including Eq. 9 in Eq. 8, gives the final formulation of the stripping cascade:

$$x_{i,j-1} = \phi y_{i,j} + (1-\phi)x_{i,j} - \nu_i \left(\frac{k_f}{k_{f,\text{ref}}} \right) \left(\frac{D}{1-D} \right) r(\boldsymbol{x}_j) \qquad (i = 1, \ldots, c-1) \qquad (j = 1, 2, \ldots, N), \tag{10}$$

where $\boldsymbol{x}_0 = \boldsymbol{x}_F$.

Equation 10 is a nonlinear, autonomous, implicit, discrete dynamical system of the form:

$$\boldsymbol{f}(\boldsymbol{x}_{j+1}, \boldsymbol{x}_j, \boldsymbol{p}) = 0, \tag{11}$$

where $\boldsymbol{x}$ is the vector of states and $\boldsymbol{p}$ is the vector of parameters. Such systems have known mathematical properties for fixed points, stability, etc. (such as Mira, 1987; Julka, 1995).

Equation 10 can be solved recursively for given values of the parameters, ϕ and D, starting with the initial condition, $\boldsymbol{x}_0 = \boldsymbol{x}_F$. The solution is a trajectory of liquid compositions for the stripping cascade.

We can also derive a model for the rectifying cascade

$$y_{i,j-1} = \phi y_{i,j} + (1-\phi)x_{i,j} - \nu_i \left(\frac{k_f}{k_{f,\text{ref}}} \right) \left(\frac{D}{1-D} \right) r(\boldsymbol{x}_j) \qquad (i = 1, \ldots, c-1) \qquad (j = 2, 3, \ldots, M), \tag{12}$$

where $\boldsymbol{y}_1 = \boldsymbol{y}_1^s$, and $\boldsymbol{y}_1^s$ is the vapor stream composition from the first flash device of the stripping cascade shown in Figure

1. The solution to Eq. 12 is a trajectory of the vapor-phase compositions along the rectifying cascade.

Equations 10 and 12 model the cocurrent stripping and rectifying cascades, respectively. For a given feed composition, these cascades are solved recursively for N, $M \to \infty$, until there is no change in successive iterates, that is, until a stable fixed point is reached.

We demonstrate the use of this model on an example and then characterize its properties in terms of fixed points and bifurcations.

Feasibility hypothesis

The flash cascade provides a two-parameter (ϕ and D) model (Eqs. 10 and 12). The iterates depend primarily on the value of D. The pinch points toward which these iterates evolve depend only on a single parameter, (Da/ϕ) (see Appendix B). Therefore, the solution structure is not dependent on the value of ϕ, and we can choose any value of ϕ (we pick $\phi = 0.5$). This simply rescales the value of Da at which bifurcations occur.

Hypothesis. The trajectories of the flash cascades lie in the feasible product regions for continuous reactive distillation.

We test this hypothesis with an example. Consider the esterification of acetic acid with isopropanol at a pressure of 1 atm:

$$\mathrm{IPA} + \mathrm{HOAc} \Leftrightarrow \mathrm{IPOAc} + \mathrm{H_2O} \tag{13}$$

We represent the kinetics by a homogeneous model:

$$r = k_f \left(a_{\mathrm{HOAc}} a_{\mathrm{IPA}} - \frac{a_{\mathrm{IPOAc}} a_{\mathrm{H_2O}}}{K_{\mathrm{eq}}} \right), \tag{14}$$

where k_f is approximately independent of temperature, $(k_f/k_{f,\mathrm{ref}}) = 1$, and the reaction equilibrium constant has a value of 8.7 in the temperature range of interest (Lee and Kuo, 1996). The VLE was modeled using the Antoine vapor-pressure equation, the NRTL equation for activity coefficients, and including vapor-phase dimerization of acetic acid. The physical-property models were taken from Venimadhavan et al. (1999, Table 3).

Solutions of Eqs. 10 and 12, the rectifying and stripping flash-cascade trajectories, can be represented in mol-fraction space (three-dimensional for the IPOAc system). However, we represent the solutions in transformed composition space, which is two dimensional for the IPOAc system [for the derivation and properties of these transformed variables, see Ung and Doherty (1995)]. This transformed composition space is a projection of a three-dimensional mol-fraction space onto a two-dimensional transformed-composition subspace for the IPOAc system. Even though the correspondence between real compositions and transformed compositions is not one-to-one in the kinetic regime, we will make use of these transforms for the following reasons: (1) ease of visualization of the trajectories, and, (2) overall mass balance for reactive systems (kinetically or equilibrium limited) can be represented with a level rule in transformed compositions. We use this property to assess feasible splits for continuous reactive distillation.

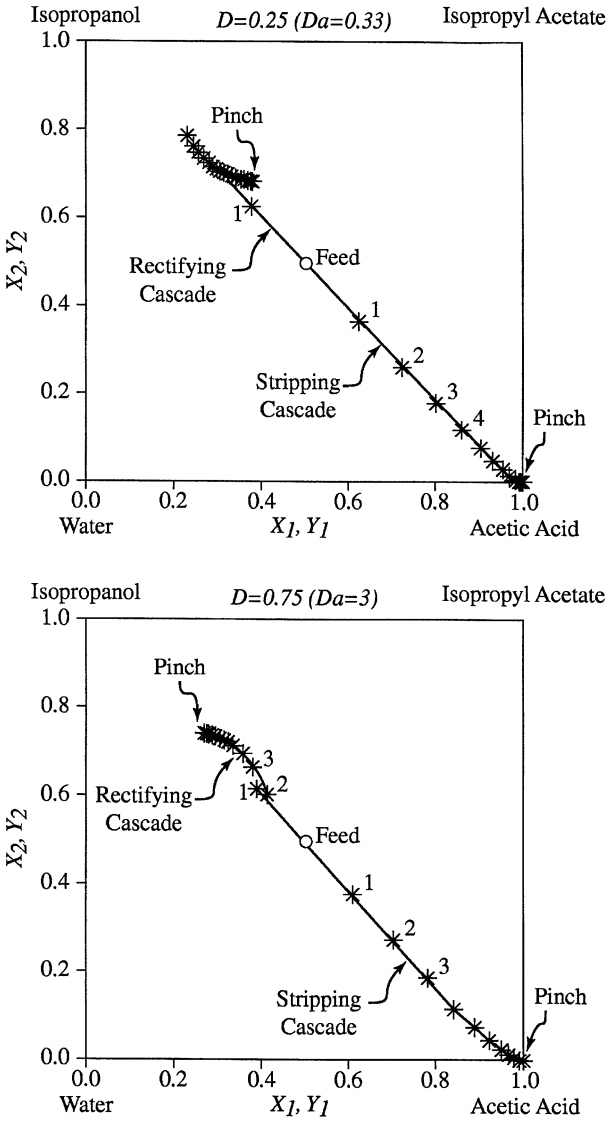

Figure 3. Rectifying and stripping cascade trajectories for a saturated liquid equimolar reactant feed for the IPOAc system at $D = 0.25$ and $D = 0.75$.

The trajectories are plotted in transformed mole-fraction space. For the stripping cascade, $X_1 = x_{\mathrm{HOAc}} + x_{\mathrm{IPOAc}}$, $X_2 = x_{\mathrm{IPA}} + x_{\mathrm{IPOAc}}$, and for the rectifying cascade, $Y_1 = y_{\mathrm{HOAc}} + y_{\mathrm{IPOAc}}$, $Y_2 = y_{\mathrm{IPA}} + y_{\mathrm{IPOAc}}$.

If we select IPOAc as the reference component, then the definition given in Ung and Doherty (1995) gives the transformed variables:

$$X_1 = x_{\mathrm{HOAc}} + x_{\mathrm{IPOAc}}$$
$$X_2 = x_{\mathrm{IPA}} + x_{\mathrm{IPOAc}}. \tag{15}$$

Similar expressions are obtained for the transformed variables in the vapor phase, Y_i.

The trajectories of the flash cascades for an equimolar feed ($x_{F,\mathrm{HOAc}} = 0.5$, $x_{F,\mathrm{IPA}} = 0.5$), are shown in Figure 3 for $D = 0.25$ and $D = 0.75$. The stripping cascade is solved recursively for this feed composition via Eq. 10 for a large number of

stages until a point is reached where the composition is essentially constant from stage to stage. This pinch point (stable node) is acetic acid. The mole fraction iterates are then converted to the transformed compositions using Eq. 15. In a similar fashion, the rectifying cascade model (Eq. 12) is solved recursively for a large number of stages until a pinch point (stable node) is reached; in this case, it is a quaternary mixture. The vapor mole fractions so obtained are then converted to transformed compositions and are shown in Figure 3.

Parametric column simulations for the IPOAc system were done with different Damköhler numbers, reflux ratios, reboil ratios, as well as total number of stages, (N_T), and feed-tray location, (f). The distillate and bottoms compositions obtained were recorded in transformed composition space.

Figure 4 compares the products obtained from column simulations with 30 stages and using different values of r and s at $D = 0.25$ and $D = 0.75$. The column feed specification is the same as that of the cocurrent flash cascade. The flash trajectories provide a good estimate of the product compositions from a continuous column. We also compared the product compositions from column simulations with the flash trajectories in mole-fraction space. We found that product compositions from column simulations surrounded the flash trajectories, in agreement with the hypothesis that the flash trajectories lie in the feasible product regions for continuous reactive distillation. We also studied various other ternary and quaternary reactive systems and found the hypothesis to hold for those systems as well (Chadda, 2001).

Note that calculating the flash trajectories at $\phi = 0.5$ does not provide the entire feasible product regions for continuous reactive distillation, but instead generates a subset of the feasible products. Selecting an iterate on the stripping cascade trajectory as a potential bottoms and an iterate on the rectifying cascade trajectory as a potential distillate does not guarantee that these products can also be obtained simultaneously from a reactive distillation column. This is simply because these product compositions may not simultaneously satisfy the overall mass balance for a reactive column. However, when the flash trajectories are used in conjunction with the lever rule for a continuous reactive column, the feasible splits for continuous reactive distillation can be quickly predicted.

Next, we derive the fixed-point criteria for the flash cascades and use bifurcation theory to propose rules to estimate feasible products.

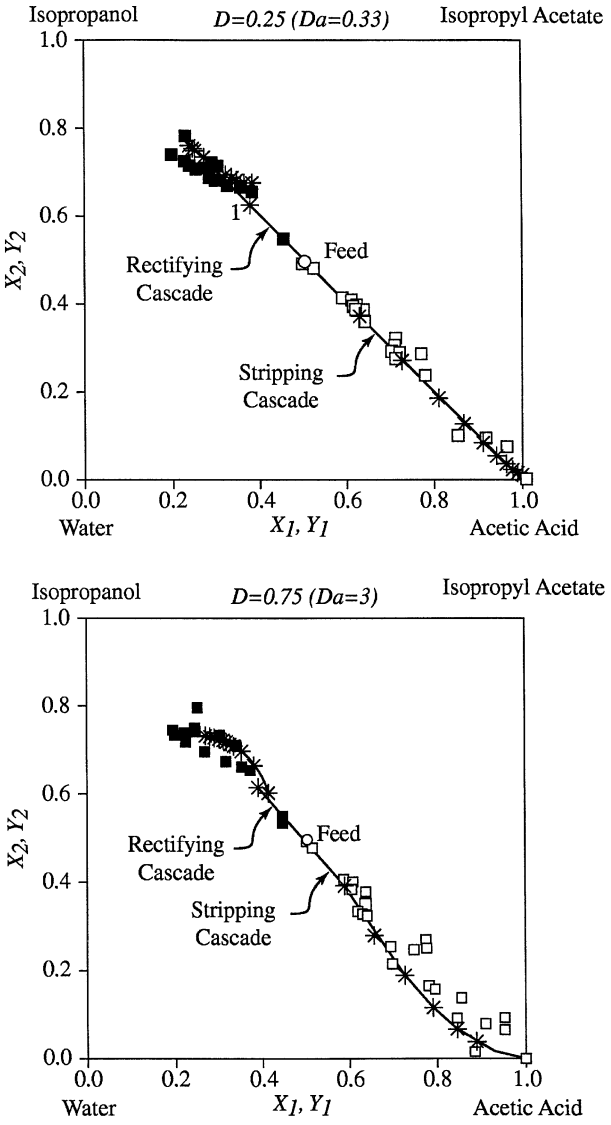

Figure 4. Feasible products from column simulations with different N_T, feed-stage location, r, s, and D recorded in transformed variable space.

The filled squares represent feasible bottoms and the open squares represent feasible distillates. The rectifying and stripping cascade trajectories from Figure 3 are also shown for comparison.

Bifurcation analysis of the flash-cascade model

The fixed points of the flash-cascade model are the solutions of Eqs. 10 and 12 for $j \to \infty$. In other words, successive liquid and vapor mole fractions reach constant values. The fixed points, $\hat{\boldsymbol{x}}$, for the stripping cascade (Eq. 10) are solutions of

$$(1-D)(\hat{x}_i - \hat{y}_i) + \nu_i \left(\frac{k_f}{k_{f,\text{ref}}}\right)\left(\frac{D}{\phi}\right) r(\hat{\mathbf{x}}) = 0 \qquad (i = 1, \ldots, c-1), \quad (16)$$

where $\hat{\boldsymbol{x}}$ and $\hat{\boldsymbol{y}}$ are in vapor–liquid equilibrium with each other.

Similarly, the fixed points, $\hat{\boldsymbol{y}}$, for the rectifying cascade (Eq. 12) are solutions of:

$$-(1-D)(\hat{x}_i - \hat{y}_i) + \nu_i \left(\frac{k_f}{k_{f,\text{ref}}}\right)\left(\frac{D}{1-\phi}\right) r(\hat{\boldsymbol{x}}) = 0 \qquad (i = 1, \ldots, c-1). \quad (17)$$

The fixed points obtained by solving Eq. 12 for a large number of iterates are stable nodes in the rectifying cascade. The same fixed points will form a subset of solutions to Eq. 17. However, to have an analogy between this work and the earlier work done in nonreactive and equilibrium-limited re-

active distillation, we rewrite Eq. 17 as

$$(1-D)(\hat{x}_i-\hat{y}_i)-\nu_i\left(\frac{k_f}{k_{f,\mathrm{ref}}}\right)\left(\frac{D}{1-\phi}\right)r(\hat{\boldsymbol{x}})=0 \qquad (i=1,\ \ldots,\ c-1), \quad (18)$$

where $\hat{\boldsymbol{x}}$ and $\hat{\boldsymbol{y}}$ are in vapor–liquid equilibrium with each other.

Equation 18 has the same fixed points as Eq. 17, *except that their stability is reversed.* Thus, a fixed point that is a stable node in Eq. 17 becomes an unstable node for Eq. 18.

The solutions for Eq. 16 and 18 behave as follows:

At $D=0$ (*the nonreactive limit*), the fixed-point criteria for both the rectifying and stripping cascades reduce to the same equation:

$$\hat{x}_i-\hat{y}_i=0 \qquad (i=1,\ \ldots,\ c-1). \quad (19)$$

Equation 19 represents the fixed-point criteria for simple distillation and also for a continuous column at total reflux and total reboil. Since there is a symmetry in the rectifying and stripping maps, we can find the fixed points for *both* the rectifying and stripping cascades from Eq. 19. Thus, in this limit, our model recovers the criterion for fixed points in the well-known limit of no reaction.

At $D=1$ (*the chemical equilibrium limit*), the fixed point criteria reduce to a single equation:

$$r(\hat{\boldsymbol{x}})=0. \quad (20)$$

Equation 20 implies that fixed points lie on the reaction equilibrium surface. Equation 20, however, is just a necessary condition; the sufficient condition for fixed points of the rectifying and stripping cascades can be written in terms of transformed variables by writing either Eq. 16 or Eq. 18 for component i and a reference component, k, and adding the two, giving:

$$\hat{X}_i-\hat{Y}_i=0 \qquad (i=1,\ \ldots,\ c-2). \quad (21)$$

The solutions of Eq. 21 are fixed points for simple reactive distillation at chemical equilibrium and also for a continuous reactive distillation at total reflux and total reboil. As in the nonreactive case, the fixed-point criteria for the rectifying and stripping cascades are the same and are given by Eq. 20 and 21. Once again our model reduces to the well-known criteria for chemical equilibrium fixed points.

For $0<D<1$ (*kinetically controlled regime*), Eq. 16 gives the fixed points of the stripping cascade and Eq. 18 the fixed points of the rectifying cascade. Therefore, in the kinetic regime, there are *different* fixed-point criteria for the rectifying and stripping cascades, a fact that has not been previously recognized. The solutions of Eq. 16 at $\phi=1$ are the fixed points for simple reactive distillation and were studied by Venimadhavan et al. (1999), but the structure of the solutions to Eq. 18 has not been reported. As we shall we, it can be quite different than for Eq. 16. Since fixed points for simple reactive distillation are equivalent to the fixed points of the stripping cascade at $\phi=1$, they can only provide information about the potential bottoms product from a continuous column. *Therefore, the distillate product composition from a continuous column for* $0<D<1$ *cannot be inferred from a knowledge of fixed points of simple reactive distillation.* It is possible, however, to estimate potential distillates from the fixed points of the rectifying flash cascade (Eq. 18). This is the key result of this article.

We are interested in investigating the fixed-point branches of the flash cascade model for $0\le D\le 1$ at $\phi=0.5$. A systematic approach is by a bifurcation analysis of the solutions, $\hat{\boldsymbol{x}}(D)$, for Eqs. 16 and 18. The starting points for the analysis are the solutions at $D=0$; to calculate these points, a homotopy continuation method by Fidkowski et al. (1993) is available. We use the mixture boiling point, $T[\hat{\boldsymbol{x}}(D)]$, to represent the solution. The branches of fixed points were calculated using the pseudoarclength continuation method in AUTO (Doedel, 1986).

For the IPOAc system, the fixed-point branches are shown (Figure 5) in bifurcation diagrams for the rectifying and stripping cascades. The left edge of the diagrams ($D=0$) represents the limit of no reaction. Here, there is a minimum boiling ternary azeotrope containing isopropanol, isopropyl acetate, and water, which is an unstable node; six intermediate boiling fixed points (all saddles); acetic acid as the heaviest species (stable node). Starting from these initial conditions, fixed-point branches are tracked for both the rectifying and stripping cascades.

The branches of interest are the unstable nodes in the rectifying bifurcation diagram and the stable nodes in the stripping cascade bifurcation diagram. These node branches are shown separately in a *feasibility diagram* (Figure 6).

The feasibility diagram provides a global view of the feasible products to expect from a continuous distillation at any rate of reaction (D). For any feed composition and for D in the range, $0\le D\le 0.395$, it is possible to obtain acetic acid as bottoms from a continuous reactive distillation. For $0.395\le D\le 1$, however, we can obtain either isopropanol or acetic acid as the bottoms product, depending on the feed composition. The potential distillates are all quaternary mixtures, with compositions that depend on D. Thus, different splits are feasible for different ranges of the Damköhler number. Conversely, any given split may or may not be feasible as the reaction rate or residence time is changed, so that the feasibility of a given separation may depend on production rates, catalyst levels, and liquid holdup. The results mean that IPOAc cannot be obtained as a pure product from a single-feed fully reactive column, no matter what rate of reaction the column is operated at.

Thus, we propose the following rule:

Rule for Feasible Products. Unstable node branches in the feasibility diagram represent potential distillates, while the stable node branches represent the potential bottoms from a continuous reactive distillation column.

Algorithm to Calculate Feasible Splits

The following algorithm generates a feasibility diagram for the flash-cascade model. It also involves calculating flash trajectories of the rectifying and stripping cascades for a given

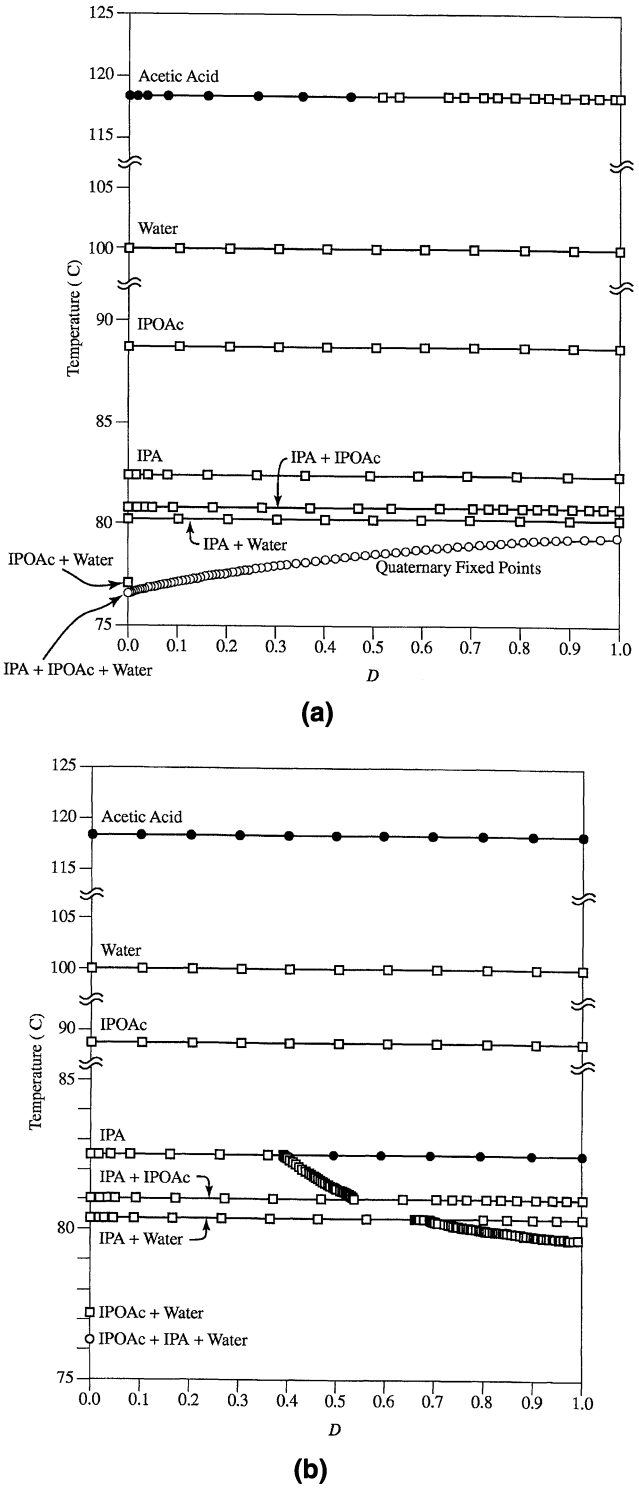

Figure 5. Bifurcation diagrams for rectifying and stripping cascades.

The filled circles denote stable node branches, open circles denote unstable node branches, and the open squares denote saddle branches.

feed composition and D, as well as the overall mass balance for a reactive column (lever rule in transformed compositions).

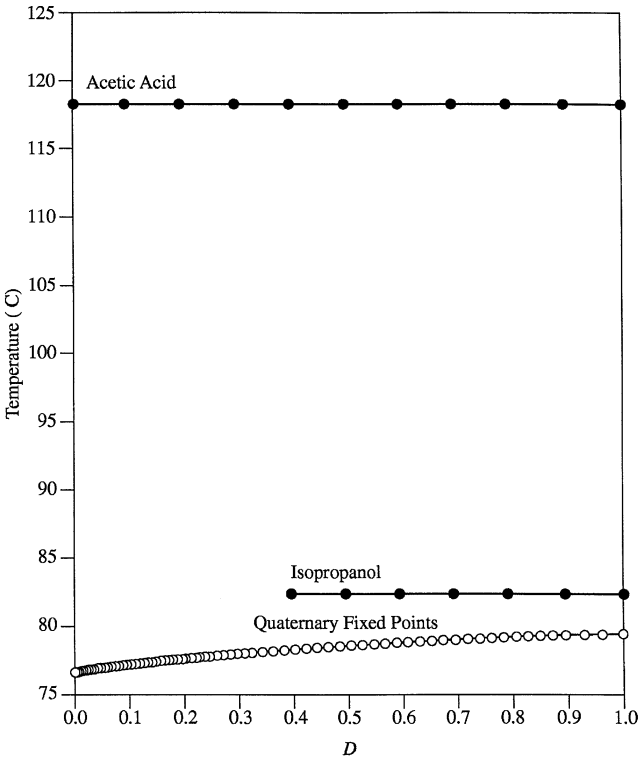

Figure 6. Feasibility diagram showing unstable and stable node branches from rectifying and stripping cascade bifurcation diagrams in Figure 5.

1. For a given mixture, at a fixed pressure, track the fixed-point branches of the rectifying and stripping cascades with respect to D. This is done by solving Eqs. 16 and 18 for $\phi = 0.5$.
2. Plot only the unstable node branches from the rectifying cascade and stable node branches from the stripping cascade on a single diagram. This is the feasibility diagram.
3. Apply the rule for sharp splits provided in the preceding section to the feasibility diagram. The unstable node branches are potential distillates, and the stable node branches are the potential bottoms from a continuous reactive distillation column.
4. Select a D at which a feasible split is desired.
5. For a given $\boldsymbol{x}_F$, solve the stripping cascade equations (Eq. 10) and the rectifying cascade equations (Eq. 12) at $\phi = 0.5$ for a large number of flash units (such as N, $M = 100$).
6. Record the stripping cascade and rectifying cascade trajectories in the transformed composition variables using the following transformation between mole fractions and the transformed variables:

$$X_i = \left(\frac{x_i \nu_k - x_k \nu_i}{\nu_k - \nu_T x_k} \right), \tag{22}$$

where k is the reference component and $i = 1, \ldots, c-2$.

7. Check if the pinch point of the rectifying cascade (potential distillate, $\hat{\boldsymbol{X}}_D$) and the pinch point of the stripping cascade (potential bottoms, $\hat{\boldsymbol{X}}_B$) simultaneously satisfy the

lever rule (overall mass balance) for the reactive distillation column. (The key idea is that the flash cascade is used to select the feasible product compositions from a reactive column that has one feed stream and two product streams, and the lever rule is imposed on those three streams alone in spite of the fact that the flash cascade itself does not obey such a level rule). For ternary systems this is equivalent to verifying if $\boldsymbol{X}_F$ lies on a straight line between $\hat{\boldsymbol{X}}_D$ and $\hat{\boldsymbol{X}}_B$. For quaternary or higher dimensional systems, this amounts to verifying the following:

$$\left(\frac{X_{F,1}-\hat{X}_{B,1}}{\hat{X}_{D,1}-X_{F,1}}\right)=\left(\frac{X_{F,i}-\hat{X}_{B,i}}{\hat{X}_{D,i}-X_{F,i}}\right)\qquad (i=1,\ \ldots,\ c-2). \tag{23}$$

If the preceding condition is satisfied, go to step 9. Else,

8. Select $\hat{\boldsymbol{X}}_B$ as the potential bottoms (respectively, $\hat{\boldsymbol{X}}_D$ as potential distillate). Find the equation of the straight line that contains $\hat{\boldsymbol{X}}_B$ and $\boldsymbol{X}_F$ (respectively, equation of the straight line that has $\hat{\boldsymbol{X}}_D$ and $\boldsymbol{X}_F$ lying on it). Next, find the intersection of this overall mass-balance line with the rectifying cascade trajectory (respectively, intersection of the straight line with the stripping cascade trajectory). The result is a feasible distillate composition in transformed variable space, $\boldsymbol{X}_D$ (respectively, bottoms composition, $\boldsymbol{X}_B$).

In case there is no intersection point, no feasible splits are possible with any of the pinch points of the flash cascade model. Select the next iterate on the flash trajectory adjacent to a pinch point as a potential product and repeat this step.

9. Convert the transformed product compositions back to mole fractions by linear interpolation of the mole fractions on adjacent stages. The distillate and bottoms compositions so obtained make up a feasible split for a given feed composition.

Initializing a column simulation is done as follows. (a) The number of stages in each section of a column are put equal to the number of stages in a flash cascade that gave the split in step 9. (b) The value of D in the flash cascade is a good estimate of the stage Damköhler number in a column simulation. This is because a flash device is a steady-state unit with a feed, a liquid output, and a vapor output like a stage in a column. (c) The estimate of the ratio of distillate flow rate to bottoms flow rate is found by using the following equation:

$$\frac{F_D}{F_B}=\left(\frac{X_{F,1}-X_{B,1}}{X_{D,1}-X_{F,1}}\right), \tag{24}$$

where F_D and F_B represent the distillate and bottoms flow rates, respectively. Using this ratio and choosing r automatically fixes s by energy balance.

Esterification Example

In this section we apply the algorithm to the IPOAc system described by Eqs. 13 and 14. Steps 1 to 3 of the algorithm have already been applied in previous sections, and the feasibility diagram is shown in Figure 6. We now decide in which regime the reactive column should be operated to get a desired product. For example, isopropanol can be obtained as a

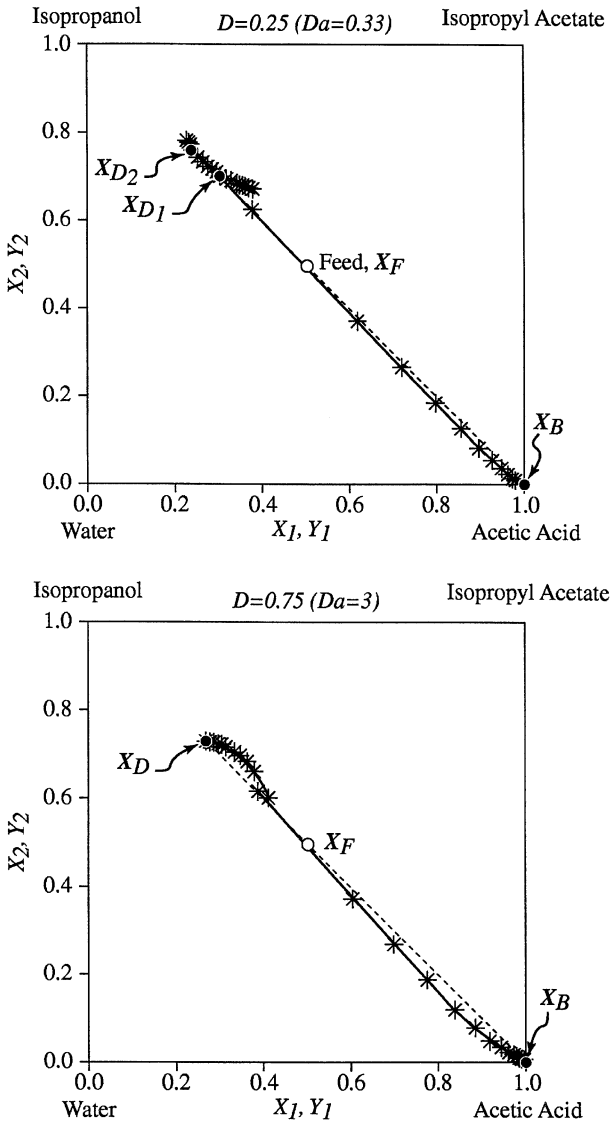

Figure 7. Feasible splits predicted by the algorithm for isopropyl acetate system at $D = 0.25$ and 0.75.

bottoms product for $0.395 \le D \le 1.0$. On the other hand, if isopropyl acetate is the desired product, we cannot get it from a single feed column containing only reactive stages. For that product we need to explore other alternatives, for example, a two-feed column and/or a hybrid column (a column with reactive and nonreactive sections), and so on.

Once we have decided the value of D at which a desired split is feasible (step 4), we solve Eqs. 10 and 12 at $\phi = 0.5$ as per step 5. The feed composition is an equimolar feed of isopropanol and acetic acid. If acetic acid is the desired product, we know from the feasibility diagram that it is possible to get it at any value of D and that it will always be a bottoms product. We solve Eqs. 10 and 12 at two different rates of reaction; $D = 0.25$ and 0.75. The rectifying and stripping cascade trajectories are shown in Figure 7 in accordance with step 6 of the algorithm. Next, we apply the lever rule (step 7 of the algorithm) and verify whether it is possible to obtain the pinch points of the flash cascades simultaneously from a

Table 1. Feasible Splits: Predicted by Algorithm vs. Column Simulations at $D = 0.25$ for Two Splits in Figure 7

Split 1			Split 2		
Mole Fraction	Algorithm Prediction	Column Simulation*	Mole Fraction	Algorithm Prediction	Column Simulation**
Distillate			*Distillate*		
HOAc	0.001	0.006	HOAc	0.0009	0.005
IPA	0.396	0.394	IPA	0.5182	0.5173
IPOAc	0.303	0.300	IPOAc	0.239	0.2387
Water	0.299	0.299	Water	0.2416	0.2400
Bottoms			*Bottoms*		
HOAc	1.0	0.999971	HOAc	1.0	0.999928
IPA	0.0	0.000004	IPA	0.0	0.000009
IPOAc	0.0	0.000008	IPOAc	0.0	0.00002
Water	0.0	0.000016	Water	0.0	0.00004
F_D/F_B	2.55	2.58	F_D/F_B	1.92	2.02

*Column design: $N_T = 30$, $f = 10$; $r = 2$; $s = 7.75$.
**Column design: $N_T = 30$, $f = 10$; $r = 2$; $s = 6.1$.

continuous reactive column. For example, at $D = 0.25$, we know from flash-cascade calculations that $\hat{X}_D = (0.382, 0.674)$ and $\hat{X}_B = (1, 0)$ for a feed composition, $X_F = (0.5, 0.5)$. Using these values, the left side of Eq. 23 is equal to 4.24 and the right side is equal to 2.87. Since the two values are not equal, we conclude that the pinch points of the flash cascades do not obey the lever rule and thus cannot be simultaneously obtained in continuous reactive distillation at $D = 0.25$. A similar result is obtained at $D = 0.75$.

In step 8, we must select one of the flash-cascade pinch points as a potential product from a continuous column. We selected the pinch point of the stripping cascade ($\hat{X}_B$) as the potential bottoms product from a reactive distillation column. Next, we make use of graphical techniques to show the application of the lever rule for the overall mass balance (although we can accomplish the same by an equation-based approach, as provided in the algorithm). We draw a straight line joining the bottoms ($\hat{X}_B$) and the feed composition (X_F). This overall mass balance line is shown in Figure 7 as a dotted line for both cases. This overall mass-balance line is extended until it intersects the rectifying cascade trajectory. The point of intersection of the rectifying cascade trajectory and the overall mass-balance line indicates a feasible split with acetic acid as bottoms (X_B) and the intersection point as the distillate (X_D). As a last step, we convert the transformed product compositions into mole fractions. The feasible split predictions from the algorithm are shown in Tables 1 and 2 for $D = 0.25$ and $D = 0.75$, respectively.

To verify that these splits are achievable in a continuous column, we performed independent column simulations for the same feed composition as in the flash-cascade model using the methods described in Huss et al. (2000). The column product compositions and column designs are compared in Tables 1 and 2 for $D = 0.25$ and $D = 0.75$, respectively. Note that the column designs provide product splits that are in good agreement with the algorithm predictions.

Table 2. Feasible Splits: Predicted by the Algorithm vs. Column Simulations at $D = 0.75$ for the Split in Figure 7

Mole Fraction	Algorithm Prediction	Column Simulation*
Distillate		
HOAc	0.0029	0.007
IPA	0.467	0.454
IPOAc	0.265	0.268
Water	0.265	0.27
Bottoms		
HOAc	1.0	0.999962
IPA	0.0	0.000002
IPOAc	0.0	0.000029
Water	0.0	0.000007
F_D/F_B	2.155	2.25

*Column design: $N_T = 30$, $f = 10$; $r = 19$; $s = 45$.

Summary of Additional Examples

We also studied other systems as follows:

A Hypothetical Ternary System: $2C \Leftrightarrow A + B$ with a Reaction Equilibrium Constant of 0.25. Component C is the heaviest and A is the lightest boiling species (relative volatilities $\alpha_{AC} = 5$ and $\alpha_{BC} = 3$). This mixture exhibits a reactive azeotrope at the limit of chemical equilibrium and a branch of kinetic pinches in the stripping section that begins at the heaviest component C at $D = 0$ and ends at the reactive azeotrope at $D = 1$, which appears as a stable node branch in the feasibility diagram. Using a parametric study we could validate that the flash trajectories at $\phi = 0.5$ lie in the feasible product regions at different rates of reaction. The bifurcation diagrams for the rectifying and stripping cascades are different. In addition, we predicted feasible splits using the algorithm described in the previous section. For example, the algorithm predicts the following sharp split at $D = 0.09$ for a pure reactant feed—distillate: $x_A = 1.0$, $x_B = 0$; bottoms: $x_A = 0.054$, $x_B = 0.124$. A column simulation for the same feed and D with $N_T = 40$, $f = 20$, $r = 10$, and $s = 0.55$ yields a distillate composition of $x_A = 1.0$, $x_B = 0$, and a bottoms composition of $x_A = 0.057$, $x_B = 0.111$.

Etherification Reaction: MeOH + Isobutene ⇔ MTBE. Since this is a nonequimolar chemistry, we used the general flash-cascade model provided in Appendix A. We verified the methodology and predicted feasible splits using the algorithm described in the previous section. For example, at $D = 0.09$, sharp split products for an equimolar reactant feed are: distillate: $x_{\text{Isobutene}} = 0.934$, $x_{\text{MeOH}} = 0.0642$; bottoms: $x_{\text{Isobutene}} = 0$, $x_{\text{MeOH}} = 1.0$. A column simulation with $N_T = 30$, $f = 15$, $r = 10$, and $s = 12.65$ yields a distillate composition of

$x_{\text{Isobutene}} = 0.931$, $x_{\text{MeOH}} = 0.055$, and a bottoms composition of $x_{\text{Isobutene}} = 0$, $x_{\text{MeOH}} = 1$.

Esterification of Methanol: MeOH + AceticAcid ⇔ MeOAc + H_2O. For this chemistry, the bifurcation diagrams for both the rectifying and stripping cascades are identical and the same as the bifurcation diagram for simple distillation provided in Venimadhavan et al. (1999, Figure 8). The feasibility diagram contains only two branches, the unstable-node branch of methanol–methyl acetate azeotrope and the stable node branch of acetic acid. Application of the rule for sharp splits leads to the conclusion that acetic acid can be obtained as a bottoms product from a continuous reactive column and/or methanol–methyl acetate azeotrope can be obtained as the distillate. Whether or not the two can be obtained simultaneously is contingent on their satisfying the lever rule (Eq. 23).

Cross Esterification: MeOH + EtOAc ⇔ MeOAc + EtOH. For this system the bifurcation diagrams for the rectifying and stripping cascades are the same, and we predicted sharp splits that were then vertified by column simulations. For example, at $D = 0.33$, sharp-split products for an equimolar reactant feed are: distillate: $x_{\text{MeOAc}} = 0.658$, $x_{\text{MeOH}} = 0.342$, $x_{\text{EtOAc}} = 0.0$; bottoms: $x_{\text{MeOAc}} = 0.008$, $x_{\text{MeOH}} = 0.007$, $x_{\text{EtOAc}} = 0.345$. A column simulation with $N_T = 30$, $f = 15$, $r = 9$, and $s = 10$ yields a distillate composition of $x_{\text{MeOAc}} = 0.655$, $x_{\text{MeOH}} = 0.344$, $x_{\text{EtOAc}} = 0.000045$, and a bottoms composition of $x_{\text{MeOAc}} = 0.0002$, $x_{\text{MeOH}} = 0.004$, $x_{\text{EtOAc}} = 0.344$.

In general, the predictions of sharp splits for different chemistries are in good agreement with column simulations. For detailed results, see Chadda (2001).

Conclusions

A flash-cascade model is developed to estimate feasible products from a continuous single-feed reactive distillation column. An important finding is that the fixed-point structures for the rectifying and stripping cascades are different for the kinetically controlled regime. The fixed-point structure of the flash cascade model is helpful in determining the reaction regime in which the column must be operated to get the desired products. We used a feasibility diagram to depict possible *sharp-split* products as a function of production rate, catalyst level, and liquid holdup. With this diagram one can quickly determine if a desired product can be obtained from a single-feed reactive column.

The proposed algorithm can be applied to any chemistry with any number of components and reactions. Moreover, it can be easily extended to multiple reaction systems including selectivity effects. One advantage of the approach is that an experimental procedure can be developed to experimentally obtain the stripping cascade and rectifying cascade trajectories. This would also be useful for mixtures for which VLE parameters are not available in the literature.

Finally, we emphasize that the algorithm should be used at the conceptual-design stage to get a good estimate of the kind of splits that are possible. The algorithm covers sharp splits, but not all possible splits.

Acknowledgment

Financial support from the National Science Foundation (Grant No. CTS-9613489) is gratefully acknowledged. The authors thank the sponsors of the Process Design and Control Center at the University of Massachusetts, Amherst, and Sean Davern of Dow-Corning in particular for helpful suggestions.

Notation

a_i = activity of i
c = total number of components
D = scaled Damköhler number, dimensionless
Da = Damköhler number, dimensionless
f = feed stage location in a continuous distillation column
F = molar flow rate
H_j = liquid holdup it unit j, mol
K_{eq} = reaction equilibrium constant
k_f = forward reaction rate constant, 1/time
$k_{f,\text{ref}}$ = forward reaction rate constant at the reference temperature
L = liquid flow rate, mol/time
P = system pressure
$M(\boldsymbol{x})$ = average molecular weight ($= \sum_{i=1}^{c} M_i x_i$)
M = index for rectifying cascade flash unit
N = index for stripping cascade flash unit
N_T = total number of stages in a continuous distillation column
$r(\boldsymbol{x})$ = driving force for the reaction
r = reflux ratio
s = reboil ratio
T = temperature
V = vapor flow rate, mol/time
$\boldsymbol{x}$ = state vector
x_i = mol fraction of i in the liquid phase
X_i = transformed mol fraction of i in the liquid phase
y_i = mol fraction of i in the vapor phase
Y_i = transformed mol fraction of i in the vapor phase

Greek letters

α_{AB} = relative volatility of A with respect to B
γ_i = liquid activity coefficient
ν_i = stoichiometric coefficient for i
ν_T = summation of all stoichiometric coefficients
ϕ_j = fraction of feed vaporized in jth flash unit

Subscripts and superscripts

0 = initial condition
B = bottoms
D = distillate
F = feed
i = component index
j = stage index for flash cascade
k = reference component
ref = reference
$\hat{}$ = pinch composition

Literature Cited

Barbosa, D., and M. F. Doherty, "Design and Minimum Reflux Calculations for Single-Feed Multicomponent Reactive Distillation Columns," *Chem. Eng. Sci.*, **43**, 1523 (1988).

Buzad, G., and M. F. Doherty, "Design of Three-Component Kinetically Controlled Reactive Distillation Columns Using Fixed-Point Methods," *Chem. Eng. Sci.*, **49**, 1947 (1994).

Buzad, G., and M. F. Doherty, "New Tools for the Design of Kinetically Controlled Reactive Distillation Columns for Ternary Mixtures," *Comput. Chem. Eng.*, **19**, 395 (1995).

Chadda, N., M. F. Malone, and M. F. Doherty, "Feasible Products for Kinetically Controlled Reactive Distillation of Ternary Mixtures," *AIChE J.*, **46**, 923 (2000).

Chadda, N., PhD Diss., Univ. of Massachusetts at Amherst (2001).

Ciric, A. R., and D. Gu, "Synthesis of Nonequilibrium Reactive Distillation Processes by MINLP Optimization," *AIChE J.*, **40**, 1479 (1994).

Damköhler, G., "Stromungs und Warmeubergangsprobleme in Chemischer Technik and Forschung," *Chem. Ing. Tech.*, **12**, 469 (1939).

Doedel, E., "AUTO: Software for Continuation and Bifurcation

Problems in Ordinary Differential Equations," Dept. of Mathematics, California Institute of Technology, Pasadena (1986).
Doherty, M. F., and G. Buzad, "Reactive Distillation by Design," *Trans. Inst. Chem. Eng.*, **70**, 448 (1992).
Espinosa, J., P. A. Aguirre, and G. A Perez, "Product Composition Regions of Single-Feed Reactive Distillation Columns: Mixtures Containing Inerts," *Ind. Eng. Chem. Res.*, **34**, 853 (1995).
Fidkowski, Z. T., M. F. Doherty, and M. F. Malone, "Computing Azeotropes in Multicomponent Mixtures," *Comput. Chem. Eng.*, **17**, 1141 (1992).
Fidkowski, Z. T., M. F. Doherty, and M. F. Malone, "Feasibility of Separations for Distillation of Nonideal Ternary Mixtures," *AIChE J.*, **39**, 1303 (1993).
Giessler, S., R. Y. Danilov, R. Y. Pisarenko, L. A. Serafimov, S. Hasebe, and I. Hashimoto, "Feasibility Study of Reactive Distillation Using the Analysis of the Statics," *Ind. Eng. Chem. Res.*, **37**, 4375 (1998).
Giessler, S., R. Y. Danilov, R. Y. Pisarenko, L. A. Serafimov, S. Hasebe, and I. Hashimoto, "Feasibility Separation Modes for Various Reactive Distillation Systems," *Ind. Eng. Chem. Res.*, **38**, 4060 (1999).
Henley, E. J., and J. D. Seader, *Equilibrium Stage Separation Operations in Chemical Engineering*, Wiley, New York (1981).
Huss, R. S., F. Chen, M. F. Malone, and M. F. Doherty, "Simulation of Kinetic Effects in Reactive Distillation," *Comput. Chem. Eng.*, **24**, 2457 (2000).
Ismail, S. R., E. N. Pistikopoulous, and K. P. Papalexandri, "Synthesis of Reactive and Combined Reactor/Separation Systems Utilizing a Mass/Heat Exchange Transfer Module," *Chem. Eng. Sci.*, **54**, 2721 (1999).
Julka, V., PhD Diss., Univ. of Massachusetts at Amherst (1995).
Lee, J. W., S. Hauan, and A. W. Westerberg, "Circumventing an Azeotrope in Reactive Distillation," *Ind. Eng. Chem. Res.*, **39**, 1061 (2000a).
Lee, J. W., S. Hauan, and A. W. Westerberg, "Graphical Methods for Reactive Distribution in a Reactive Distillation Column," *AIChE J.*, **46**, 1218 (2000b).
Lee, L.-S., and M.-Z. Kuo, "Phase and Reaction Equilibria of the Isopropanol-Acetic Acid-Isopropyl Acetate Water System at 760 mm Hg," *Fluid Phase Equilib.*, **123**, 147 (1996).
McGregor, C., D. Glasser, and D. Hildebrandt, "Process Synthesis of a Reactive Distillation System Using Attainable Region Results," *Distillation and Absorption, Inst. Chem. Eng. Symp. Ser.*, **142**, 663 (1997).
Mira, C., *Chaotic Dynamics*, World Scientific, Singapore (1987).
Nisoli, A., M. F. Malone, and M. F. Doherty, "Attainable Regions for Reaction and Separation," *AIChE J.*, **43**, 374 (1997).
Okasinski, M. J., and M. F. Doherty, "Design Method for Kinetically Controlled, Staged Reactive Distillation Columns," *Ind. Eng. Chem. Res.*, **37**, 2821 (1998).
Papalexandri, K. P., and E. N. Pistikopoulous, "Generalized Modular Representation for Process Synthesis," *AIChE J.*, **42**, 1010 (1996).
Rev, E., "Reactive Distillation and Kinetic Azeotropy," *Ind. Eng. Chem. Res.*, **33**, 2174 (1994).
Rooks, R. E., V. Julka, M. F. Doherty, and M. F. Malone, "Structure of Distillation Regions for Multicomponent Azeotropic Mixtures," *AIChE J.*, **44**, 1382 (1998).
Safrit, B. T., and A. W. Westerberg, "Synthesis of Azeotropic Batch Distillation Separation Systems," *Ind. Eng. Chem. Res.*, **36**, 1841 (1997).
Stichlmair, J. G., and J. R. Herguijuela, "Separation Regions and Processes of Zeotropic and Azeotropic Ternary Distillation," *AIChE J.*, **38**, 1523 (1992).
Thiel, C., K. Sundmacher, and U. Hoffmann, "Residue Curve Maps for Heterogeneously Catalysed Reactive Distillation of Fuel Ethers MTBE and TAME," *Chem. Eng. Sci.*, **52**, 993 (1997).
Ung, S., and M. F. Doherty, "Synthesis of Reactive Distillation Systems with Multiple Equilibrium Chemical Reactions," *Ind. Eng. Chem. Res.*, **34**, 2555 (1995).
Venimadhavan, G., M. F. Malone, and M. F. Doherty, "Effect of Kinetics on Residue Curve Maps for Reactive Distillation," *AIChE J.*, **40**, 1814 (1994), [Correction: *AIChE J.*, **41**, 2613 (1995)].
Venimadhavan, G., M. F. Malone, and M. F. Doherty, "Bifurcation Study of Kinetic Effects in Reactive Distillation," *AIChE J.*, **45**, 546 (1999).
Wahnschafft, O. M., J. W. Koehler, E. Blass, and A. W. Westerberg, "The Product Composition Regions of Single-Feed Azeotropic Distillation Columns," *Ind. Eng. Chem. Res.*, **31**, 2345 (1992).

Appendix A: General Flash Cascade Model

The model developed in this article is applicable to equimolar chemistries. If the chemistry is nonequimolar, however, it is advantageous to use parameters defined in terms of mass rather than moles. The reason is that with mass-based parameters we can define a vapor-mass fraction ϕ_m that is bounded between 0 and 1 and is not a function of conversion. The resulting framework for the stripping cascade has been derived by Nisoli et al. (1997) using the same assumptions as used in this article. These equations, derived and listed as Eq. 9 in Nisoli et al. (1997), are given below:

Stripping cascade:

$$(x_{i,j} - x_{i,j-1}) = \phi_m \frac{M(\boldsymbol{x}_{j-1})}{M(\boldsymbol{y}_j)}(x_{i,j} - y_{i,j}) + (\nu_i - \nu_T x_{i,j})\left(\frac{k_f}{k_{f,\mathrm{ref}}}\right)\left(\frac{D}{1-D}\right)\frac{M(\boldsymbol{x}_{j-1})}{M(\boldsymbol{x}_j)} r(\boldsymbol{x}_j) \quad (i = 1, \ldots, c-1) \qquad (j = 1, 2, \ldots, N), \tag{A1}$$

where $\boldsymbol{x}_0 = \boldsymbol{x}_F$.

The corresponding model for the rectifying cascade is

$$(x_{i,j} - y_{i,j-1}) = \phi_m \frac{M(\boldsymbol{y}_{j-1})}{M(\boldsymbol{y}_j)}(x_{i,j} - y_{i,j}) + (\nu_i - \nu_T x_{i,j})\left(\frac{k_f}{k_{f,\mathrm{ref}}}\right)\left(\frac{D}{1-D}\right)\frac{M(\boldsymbol{y}_{j-1})}{M(\boldsymbol{x}_j)} r(\boldsymbol{x}_j) \quad (i = 1, \ldots, c-1) \qquad (j = 2, 3, \ldots, M), \tag{A2}$$

where $\boldsymbol{y}_1 = \boldsymbol{y}_1^s$.

It should be noted here that the dimensionless quantities, D and ϕ_m is these equations are defined with respect to mass flows and mass holdups. In the preceding equations, a new quantity, $M(\boldsymbol{x})$, is introduced that is the average molecular weight, and appears as a consequence of using mass variables.

$$M(\boldsymbol{x}) = \sum_{i=1}^{c} M_i x_i. \tag{A3}$$

Similar definitions apply to $M(\boldsymbol{y})$. Equations A1 and A2 reduce to Eqs. 10 and 12 when $\nu_T = 0$.

The fixed-point criterion for the stripping cascade (Eq. A1) is obtained when $(\boldsymbol{x}_j - \boldsymbol{x}_{j-1}) = 0$ for the limit when $N \to \infty$:

$$(1-D)\frac{M(\hat{\boldsymbol{x}})}{M(\hat{\boldsymbol{y}})}(\hat{x}_i - \hat{y}_i) + (\nu_i - \nu_T \hat{x}_i)\left(\frac{k_f}{k_{f,\mathrm{ref}}}\right) \times \left(\frac{D}{\phi_m}\right) r(\hat{\boldsymbol{x}}) = 0 \qquad (i = 1, \ldots, c-1). \tag{A4}$$

In similar fashion, the fixed-point criterion for the rectifying cascade (Eq. A2) is obtained when $(y_j - y_{j-1}) = 0$ for the limit when $M \to \infty$:

$$(1-D)\frac{M(\hat{\boldsymbol{x}})}{M(\hat{\boldsymbol{y}})}(\hat{x}_i - \hat{y}_i) - (\nu_i - \nu_T \hat{x}_i)\left(\frac{k_f}{k_{f,\mathrm{ref}}}\right) \times \left(\frac{D}{1-\phi_m}\right) r(\hat{\boldsymbol{x}}) = 0 \qquad (i = 1, \ldots, c-1). \quad \text{(A5)}$$

The equations in this Appendix can be used to predict feasible sharp splits for any chemistry using the algorithm described in the article.

Appendix B: Fixed Points of a Two-Parameter Flash-Cascade Model Depend Only on a Single Parameter

Fixed points, $\hat{\boldsymbol{x}}$, for the two-parameter (ϕ and D) stripping cascade model (Eq. 10) are the solutions of Eq. 16. This equation can also be written as:

$$(\hat{x}_i - \hat{y}_i) + \nu_i\left(\frac{k_f}{k_{f,\mathrm{ref}}}\right)\left(\frac{\frac{D}{1-D}}{\phi}\right) r(\hat{\boldsymbol{x}}) = 0 \qquad (i = 1, \ldots, c-1). \quad \text{(B1)}$$

Equation 9 provides a relation between the parameters D and Da. Incorporating Eq. 9 in Eq. B1 gives

$$(\hat{x}_i - \hat{y}_i) + \nu_i\left(\frac{k_f}{k_{f,\mathrm{ref}}}\right)\left(\frac{Da}{\phi}\right) r(\hat{\boldsymbol{x}}) = 0 \qquad (i = 1, \ldots, C-1). \quad \text{(B2)}$$

The fixed-point structure of the stripping cascade model depends on a single parameter, Da/ϕ. Thus, the solution structure of the model is independent on any particular value of ϕ, and any value of ϕ can be chosen for representing the cascade. Various values of ϕ simply rescale the value of Da at which bifurcations occur. For example, Figure 12 in Venimadhavan et al. (1999) is the bifurcation diagram for the stripping cascade at $\phi = 1$ for the isopropyl acetate system. This diagram is equivalent to Figure 5b in this article, which was calculated at $\phi = 0.5$. Any point on Figure 12 can be represented on Figure 5b, or vice versa, by using the following relation:

$$Da^* = 2\,Da, \quad \text{(B3)}$$

where Da^* is defined as in Venimadhavan et al. (1999). A similar pattern holds for the rectifying cascade model.

Manuscript received Feb. 28, 2000, and revision received Sept. 5, 2000.